TEXTILES JOURNAL OF TEXTILES AND POLYMERS

Part A: English Edition

Journal of Textiles and Polymers

Vol. 10, No. 3, 43-53, July 2022

https://doi.org/10.48302/jtp.2022.170705

ITAST Journal of Textiles and Polymers

ORIGINAL PAPER

A Model for Fabric Compressibility and Compressed Fabric Cover Factor Using Response Surface Method

Reyhaneh Sarpanahi, Mohsen Hadizadeh*, Zeynab Soltanzade, and Saeed Fatahi

Received: 19 August 2022, Accepted: 3 April 2023

Abstract- **Fabric compressibility has a significant effect on the application, comfort, quality, and thermal properties of the fabric. Lateral compression affects the diameter of the yarns and fabric density, which causes a change in the cover factor (CF). The purpose of this paper is to investigate fabric compressibility, the cover factor, and the cover factor variation in compressed states. In this research, woven fabrics were produced with different weft density and different weft materials (polyester and viscose). The compression test was conducted at different speeds and the fabric was filmed at the same time. The density and the diameter of the warp and weft yarns, as well as the CF were extracted by image processing using video pictures. Then the fabric compressibility, CF, and, CF Variation (CFV) were modeled using the response surface method (RSM). The results obtained in the study clearly showed these models are acceptable with a high correlation. According to this model, with increasing pressure and decreasing density, fabric compressibility and CFV often increase. The compression variation range and CF were greater in polyester fabrics than in viscose fabrics by changing weft density.**

Keywords**: fabric compressibility, cover factor, warp and weft density, image processing, response surface method**

I. INTRODUCTION

Compression affects the softness of the fabric, and softness is considered as the opposite of firmness or hardness [1]. Also, comparing subjective sensory responses from wear tests and objectively measured mechanical properties, it is found that the subjective ratings of clothing stiffness are related to three types of mechanical properties, one of which is the compression properties of the fabric [1]. The relationship between softness and compression is significant for woven and non-woven fabrics, and it has been found that the higher the compressibility, the softer the fabric [2]. Generally, compression properties are important in final application, type of usage, softness, handling, bending quality, tearing, drape, and overall quality [3].

Ji and Lee (2016) tested the mechanical properties of the fabric, including the compressive properties, to examine the softness and flexibility of the woven fabrics [4]. Hu *et al.* (2007) employed the finger-fabric finite element model and showed that the compression modulus affects fabric softness [5]. Moreover, they examined the differences in sensory and mechanical analysis on fabric softness by compression testing, which could indicate the importance of compression testing in fabric softness testing [6].

Various factors affect fabric compressibility including types of fiber, yarns, fabric structures, and finishing operations [7,8]. Eryuruk (2019) investigated the compressive properties of denim fabrics with different properties. She found the highest values of compressive resilience observed for denim fabric increased with elastin [9]. Özer *et al.* (2020) investigated the compressibility and thermal properties of different multilayer mattresses. They observed that as the thickness and weight of the layers increased, the thickness, compression, and recovery characteristics of the samples improved [10].

Warp and weft yarns' diameter and density are components of fabrics that determine CF, which is an important factor in textiles [11]. Researchers have managed to determine the effects of cover factor (CF) on the needle cutting index [12], light reflection [13], permeability [14],

R. Sarpanahi, M. Hadizadeh, Z. Soltanzade, and S. Fatahi
Department of Textile Engineering, Yazd University, P.O. Box 89195-741, Yazd, Iran.

Correspondence should be addresses to M. Hadizadeh
e-mail: hadizadeh@yazd.ac.ir

the thermal resistance of a fabric [11], and so on. It has been shown that by changing yarn count and density, CF behavior also changes.

The importance of the effect of the compression factor on the cover factor can be examined in the sitting area of clothes, carpets, rugs, shoe insoles, car seat covers, socks, and in contact with two or more clothes. It is certain that the fewer the cover factor, the more heat, odor, moisture, and air permeability through the clothes [11,14,15].

Vision systems have been applied in many textile evaluation areas with the image processing technique having the potential to measure the details. This technique is very efficient to calculate the CF and density [16,17]. Shady *et al.* (2012) studied the Wiener filter and explained its equations [18]. Using a Wiener filter, each picture can decompose into two sub-images that include warp or weft yarns direction [18,19].

Statistically, the response surface method consists of mathematical methods that correlate to one or more response variables and one or more independent variables [20,21]. The RSM has been identified as an acceptable method, compared to traditional modeling techniques [21].

There are many designs available for fitting the second-order model, the most popular of which is the central composite design (CCD) [22]. Using RSM, researchers have already investigated a variety of areas such as predicting air permeability and light transmission [14] as well as optimizing the polymerization conditions, color strength, and crease recovery angle [23,24] so the RSM can be used more in the textile industry [25].

To the best of the researchers' knowledge, no significant has, to the date, been conducted using the RSM method to determine the cover factor, to check it under pressure, and to evaluate with compressibility.

In the present study, the cover factor of compressed fabric is measured using image processing. Using the response surface method, it has been tried to find the model for the relationship between variables such as fabric pressure, strength tester speed, weft density, and weft material and fabric compressibility, cover factor, and cover factor variation in compressed states.

II. THEORETICAL

Fabric compressibility is a division of variation of thickness to initial thickness. Relative fabric compressibility is calculated according to Eq. (1) [26]:

$$\mathrm{RFC} = \frac{h_0 - h_m}{h_0}.100 \tag{1}$$

where RFC is relative fabric compressibility under certain pressure, h_m denotes fabric thickness under certain pressure, and h_0 is fabric initial thickness.

In this paper, CF is obtained with image processing by calculating the diameter and distance between two yarns according to Eq. (2). The relationship between the density and the distance between the two threads is given in Eq. (3) [27]:

$$\mathrm{CF} = \frac{p_1 d_2 + p_2 d_1 - d_1 d_2}{p_1 p_2} \tag{2}$$

$$P = \frac{1}{\text{density}} \tag{3}$$

where p_1 and p_2 denote the distance between two warps and wefts and d_1 and d_2 denote the diameter of warp and weft, respectively.

In this paper, the CF at the moment when no pressure is applied to the fabric (initial CF) is also calculated by image processing and cover factor variation (CFV) is obtained from Eq. (4):

$$\mathrm{CFV} = \frac{CF_2 - CF_1}{CF_1} \times 100 \tag{4}$$

where CF_1 is initial CF and CF_2 is CF of compressed fabric under certain pressure.

The present study applied the second-order model and the central composite design (CCD). The RSM results are shown by 3D plots or a function of the variables. It is modeled using two types of approximating functions; first and second-order models are shown in Eqs. (5) and (6) [28], respectively:

$$y = \beta_0 + \sum_{i=1}^{n} \beta_i X_i \tag{5}$$

$$y = \beta_0 + \sum_{i=1}^{n} \beta_i X_i + \sum_{i=1}^{n} \beta_{ii} X_i^2 + \sum\sum_{i<j}^{n} \beta_{ij} X_i X_j + \varepsilon \tag{6}$$

where Y is the responding variable, β_0 denotes the intercept of the regression function, β_i shows the regression coefficient and X_i is the independent variable. β_{ii} is the curvature term of the independent variable and β_{ij} is the interaction coefficient between variables X_i and X_j.

III. EXPERIMENTAL

A. Materials

Samples were weaved with a Sulzer Rapier weaving Machine. Two types of weft yarn, polyester spun yarn and viscose yarn, were used with a weft yarn count of 30/2 Ne. The warp yarn count of all samples was 30/2 Ne with a warp density of 21.6 cm^{-1} on the weaving Machine. Warp types were polyester/viscose and all samples had the plain weave. Table I shows the types of fabrics.

TABLE I
SPECIFICATIONS OF THE FABRICS USED

Fabric code	Weft material	Weft density (cm^{-1})
PE_1	Polyester	11.50
PE_2	Polyester	18.88
PE_3	Polyester	26.26
V_1	Viscose	11.50
V_2	Viscose	18.88
V_3	Viscose	26.26

B. Procedures

In this paper, the strength tester of model MICRO 350 was used, which was set in compression mode. The surface of the compressed piece was 5×5 cm^2. A glass plate was also used on which fabric samples were put. A drilled metal plate and a microscopic camera were placed under the glass plate. Fig. 1 shows the locations of the components. The microscopic camera was characterized with a resolution of 135 pixels per cm. Experiments were carried out with a strength tester variable speed.

Images were selected from the film of the camera. The images were processed using MATLAB software and in

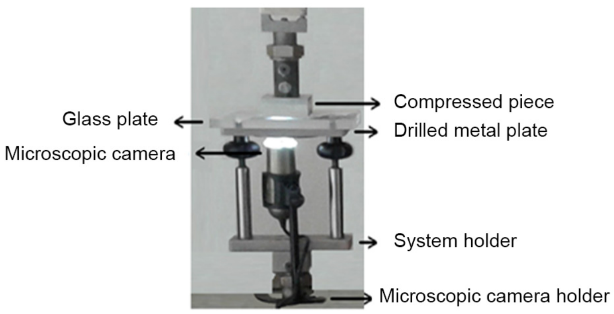

Fig. 1. Location of components.

each image, the diameter of warp and weft, the distance between two warps and two wefts, and the CF were calculated. The initial thickness was obtained with the Shirley Fabric Thickness Tester according to ASTM D 1777-664.

The RGB image was converted to a gray image. To achieve perfect images, Medium and Wiener filters were used, which determine warp direction. The warps of the fabric in the processed image (Fig. 2b) are identified as bright lines, and the change of light in the image is used to count the number of warps. By counting the number of pixels between the beginning of the first warp and the last pixel of the last yarn and dividing it by the counted number of warps, the distance between the two warps is obtained. Then, p_1 value is calculated for each row separately, and the maximum value of p_1 is used in calculations. To calculate the diameter, the images were binary in a new way. In each row in Fig. 2b, the maximum, minimum and average of numbers in the starting point of yarn, stored in the step of calculating the distance between two yarns, to the end of the next yarn were calculated. In this method, if the numbers in gray image are greater than average, the number is changed to 1, and numbers smaller than average are changed to zero (Fig. 2d). The same steps were done for the weft yarn by rotating the image. The flow chart of image processing operation is shown in Fig. 3.

Fig. 2a is a gray image fabric under 0.5 $gf.cm^{-2}$ pressure and speed loading 1 $mm.min^{-1}$. Figs. 2b and 2c show filtered versions of Fig. 2a with medium and wiener filters in the warp and weft direction, respectively. Figs. 2d and 2e show binary images of Figs. 2b and 2c, and Fig. 2f shows sum of binary pixels of each row and column of Figs. 2d and 2e, which means CF.

In the RSM, using appropriate experimental design,

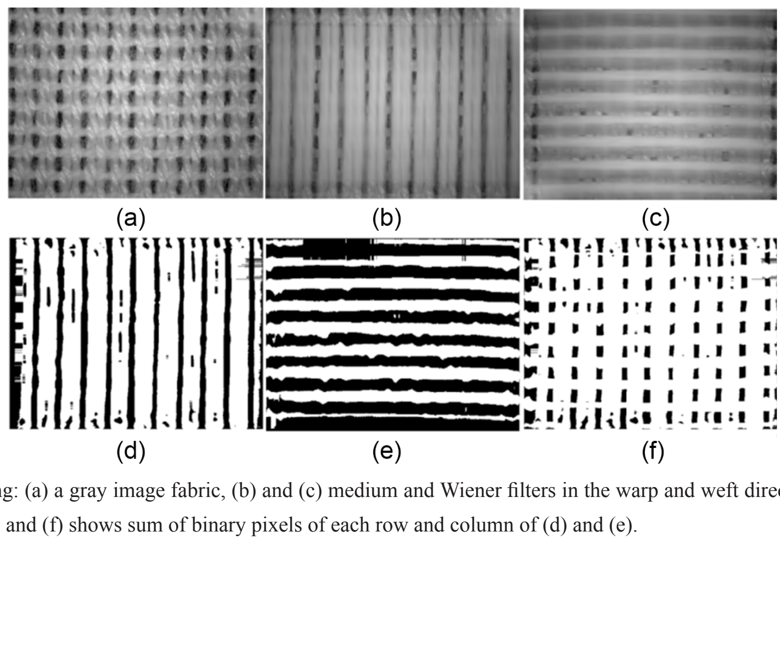

Fig. 2. Steps of image processing: (a) a gray image fabric, (b) and (c) medium and Wiener filters in the warp and weft direction respectively of (a), (d), and (e) binary images of (b) and (c), and (f) shows sum of binary pixels of each row and column of (d) and (e).

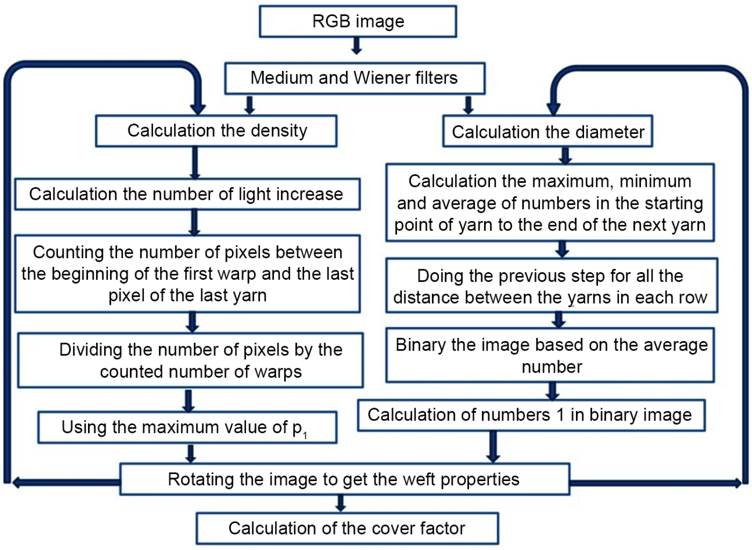

Fig. 3. Flow chart of image processing operation.

it has been tried to find an estimate for interactions, and the multi-dimensional shape of the response surface. Sustainability is the concept of minimizing the effects of secondary or non-controlling variables [29].

In this study, a face-centered central composite design (CCF design) was applied to analyze the four important variables with α=±1, using Design-Expert 10.0.7 software. The negligible effects in the model were eliminated to make the model smaller and simpler. Table II describes the independent variables and their levels.

IV. RESULTS AND DISCUSSION

Fig. 4 presents the outputs of MATLAB software which are an average of 4 samples in each state. It shows the diameter of the warp and weft and the distance between two warps and two wefts. As clearly seen in Fig. 4, with the increase in lateral pressure, the diameter of the yarns increases because by applying force, the fibers in the yarn are moved and the air between them is removed. As a result, the yarn becomes flat and the diameter of the yarn increases. This increase is more visible in fabrics with lower density because the fibers have more space to move.

According to Fig. 4, with the increase in test speed, no significant change has been made in the diameter and the distance between the yarns.

The RSM was applied to visualize the effect of four independent variables (weft density, fabric pressure, strength tester speed, and weft material) on the response (compressibility, CF, and CFV).

To evaluate the validity of the model, as shown in Fig. 5, the assumption of normality was checked. Fig. 6 shows the residual versus predicted plots. This plot tests the assumption of constant variance. The plot shows a random scatter. The predicted and observed responses are shown in Fig. 7. The closer are the points to the line, the more accurate is the prediction. Fig. 7 shows that the RSM was able to predict the actual data. The variance of the data is stated in sections 4.1 and 4.2. The color of the bullets in Figs. 5, 6, and 7 shows the value of the answer; the red color has a higher value and the blue color has a lower value.

A. Compressibility

Given fabric thickness in the compressed state and using

TABLE II
THE APPLIED EXPERIMENTAL PARAMETERS AND THEIR LEVELS

Independent variables	Definition	Code		
		-1	0	1
A	Weft densities (cm^{-1})	11.5	18.88	26.26
B	Fabric pressure ($gf.cm^{-2}$)	98	366	634
C	Strength tester speed ($mm.min^{-1}$)	1	7	13
D	Weft material	Viscose		Polyester

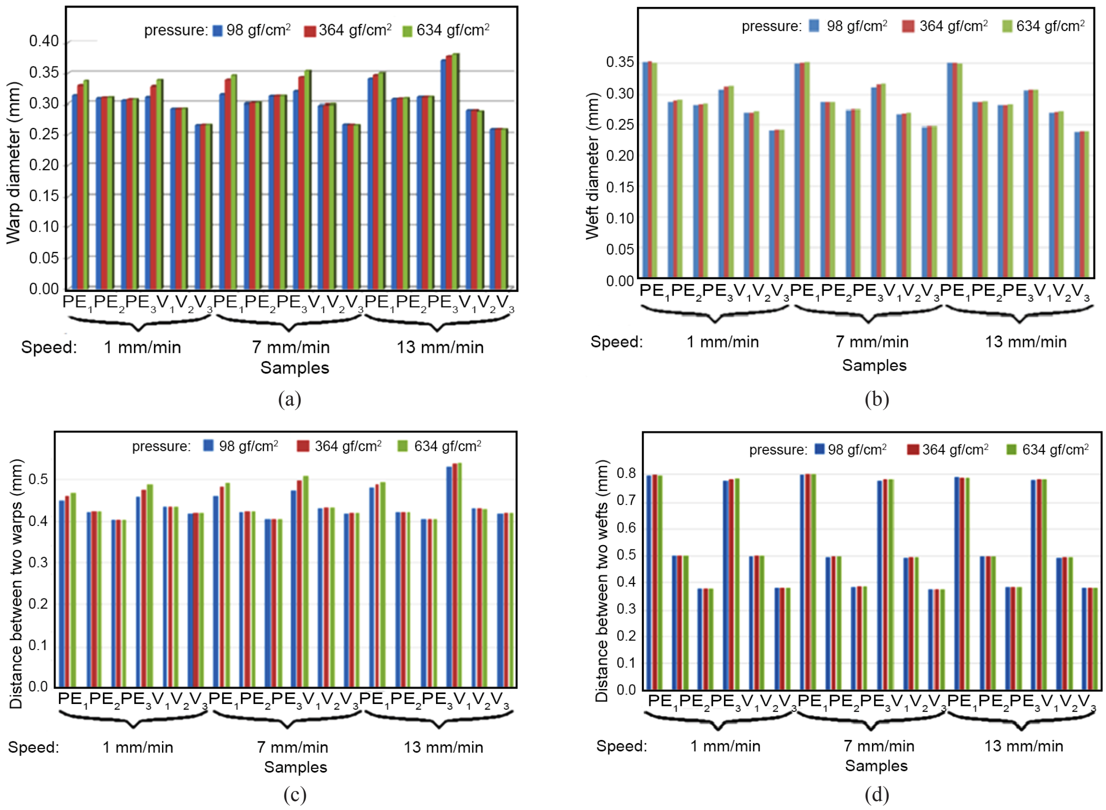

Fig. 4. Mean results obtained from outputs of MATLAB software: (a) warp diameter, (b) weft diameter (c), distance between two warps, and (d) distance between two wefts.

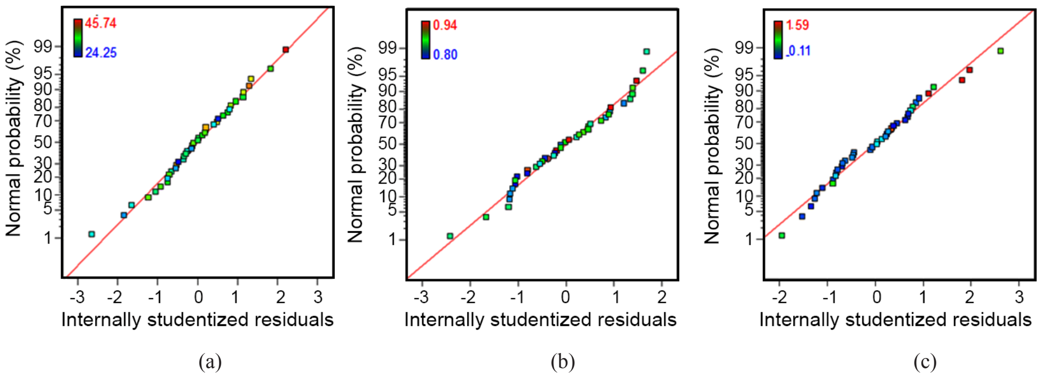

Fig. 5. Normal plots of residual: (a) fabric compressibility, (b) CF, and (c) CFV.

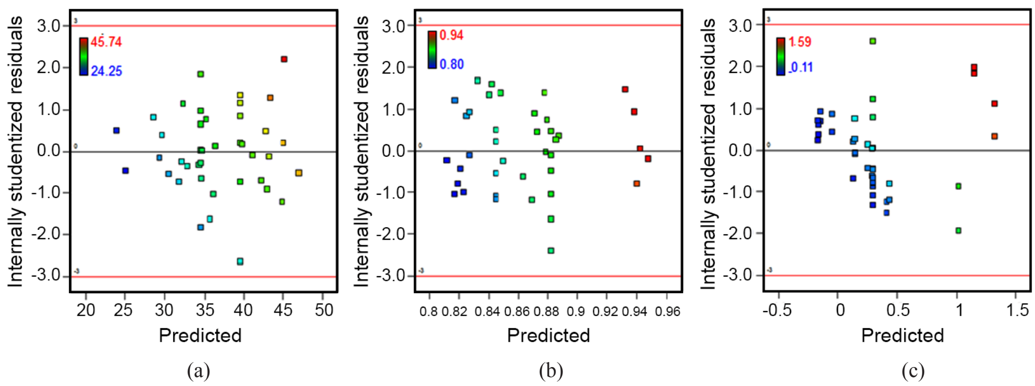

Fig. 6. Residual versus predicted plots: (a) fabric compressibility, (b) CF, and (c) CFV.

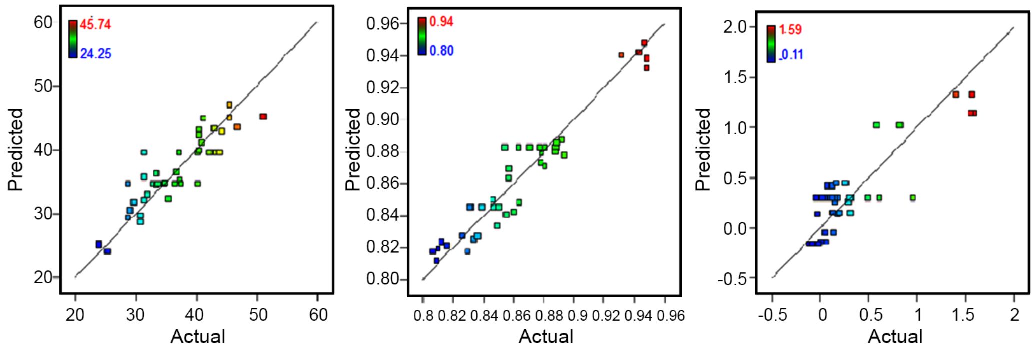

(a) (b) (c)

Fig. 7. Actual values versus predicted plots: (a) fabric compressibility, (b) CF, and (c) CFV.

Eq. (1), fabric compressibility can be calculated. The ANOVA results in Table III show the significance of the model as well as the effects of weft density, fabric pressure, weft material, the interaction of density and material, the interaction of speed and material, density squared and speed squared on fabric compressibility at 5% level of significance. The significance of each term was determined by P-value (Prob>F), as listed in Table III. In compressibility, the "lack of fit F-value" of 0.35 compares the residual error with the pure error from replicated design points. The non-significant lack-of-fit showed that the model was valid. Index statistics, R-squared coefficient, Adj R-Squared, and Pred R-squared values were 0.77, 0.71, and 0.65, respectively. The "adjusted R-squared" was as close to the "predicted R-squared" as one might normally expect. A quadratic model was suggested and the compressibility was described with this model. The model equation in terms of coded factors for compressibility is presented in Eq. (7):

$$\begin{aligned} RFC = 37 - 0.52*A + 4.79*B - 0.67*C + 2.25*D - 1.88*AB \\ +4.16*AD + 1.63*CD - 3.15*B^2 \end{aligned} \quad (7)$$

where A, B, C, and D are weft density, fabric pressure, strength tester speed, and weft material, respectively.

3D plots were drawn to study the interaction among the different independent variables and their corresponding effects on the response. Figs. 8a and 8b show the relationship between pressure and weft density and fabric compressibility in polyester fabrics (samples with polyester weft) and viscose fabrics (fabrics with viscose weft), respectively. They show that the compressibility variation range is greater in polyester fabrics compared to viscose fabrics.

By applying pressure, force is applied to overcome the

TABLE III
RESULTS OF RESPONSE SURFACE QUADRATIC MODEL FOR FABRIC COMPRESSIBILITY

Source	Sum of squares	Degrees of freedom	Mean square	F-value	P-value	Characteristics
Model	1218.90	8	152.36	14.65	< 0.0001	Significant
A-density	44.32	1	44.32	4.26	0.0474	
B-pressure	557.12	1	557.12	53.58	< 0.0001	
C-speed	11.56	1	11.56	1.11	0.2999	
D-material	253.48	1	253.48	24.38	< 0.0001	
AD	112.62	1	112.62	10.83	0.0025	
CD	34.47	1	34.47	3.31	0.0783	
A^2	134.62	1	134.62	12.95	0.0011	
C^2	187.40	1	187.40	18.02	0.0002	
Residual	322.32	31	10.40			
Lack of fit	137.56	21	6.55	0.35	0.9783	Not significant
Pure error	184.75	10	18.48			
Cor total	1541.22	39				

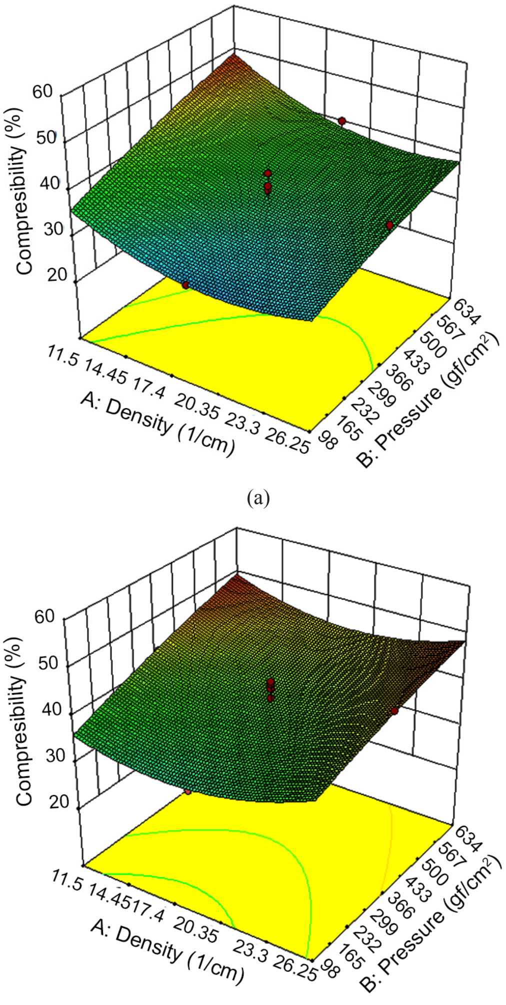

Fig. 8. Relationship of pressure and weft density with fabric compressibility in speed of 7 mm/min: (a) polyester fabrics and (b) viscose fabrics.

static friction, making the yarn and fibers slip and move within the yarn. Static friction increases with increasing pressure in the fabric [31], so more force must be expended to reduce the thickness. When there is no space for the yarns and fibers to move, the fibers exert force on each other to reduce the thickness of the fabric. In general, compressibility increases with increasing pressure, as can be seen in Fig. 8. It also shows that the difference in weft material is better determined at higher densities. At high fabric densities, there is not enough space for the fibers to move, so they exert force on each other, with different materials producing different amounts of deformation.

It can be implied from Table III that the fabric material has an interaction effect on the weft density and speed, which means that different weft materials can have different effects on compressibility at different weft densities and speeds.

In polyester fabrics, compressibility decreases with increasing the density, while in viscose fabrics, compressibility first decreases and then increases, which probably can be attributed to the percentage of air volume between the two types of fabric and the kind of fibers. Therefore, the effect of spinning, type of fiber, etc. can be further investigated.

B. CF and CFV

As mentioned, the CF of samples at Specified pressure was calculated by image processing using the image taken by the camera and then the data were analyzed by software using RSM. Table IV lists the significance of each term, determined by the P-value. According to Table IV, it is found that the model is significant and that weft density, strength tester speed, weft material, and Interaction of weft density and weft material are effective in CF at a 5% level of significance. The non-significant lack-of-fit showed that the model was valid. In CF, the “lack-of-fit F-value” of 1.36 compares the residual error to the pure error from replicated design points. Index statistics, R^2, R^2 adjust, and predicted R^2 values were 0.92, 0.91, and 0.89, respectively. The 2FI model was suggested and the CF was described with this model. The model equation is presented in Eq. (8):

$$\begin{aligned} CF = {} & 0.86 + 0.42\times10^{-1}\times A + 2.97\times10^{-3}\times B - 4.82\times10^{-3}\times C \\ & -0.19\times10^{-1}\times D - 0.16\times10^{-1}\times AD \end{aligned} \quad (8)$$

3D plots were drawn in Fig. 9 to study the interaction among the strength tester speed and weft density of different weft materials and their corresponding effect on the response. According to the ANOVA table, as the density of the weft changes, the CF changes in polyester fabrics are greater than in viscose fabrics. It can be seen from Fig. 9 that as the weft density increases, the CF increases as well, which has also been confirmed in the literature [13,14]. At low densities, the difference in weft material is very small, but at higher weft densities, the difference is greater. As mentioned in section 4.1, due to the lack of space for the fibers to move, they exert force on each other and the difference in the material of the fabric causes different deformations. Table IV shows that weft material and weft density interact with each other, and the cover factor of different materials will be different at each weft density. As the speed increases, the cover factor decreases. In high speeds, the fabrics have less time to change their shape and tend to retain their original shape.

CFV was also analyzed by RSM, and it is shown from Table V that the pressure, density, speed, interaction of density and pressure, squared density, squared pressure, and squared speed at a 5% level of significance were significant in the model. In CFV, the “lack of fit F-value” was 0.7, and the non-significant lack-of-fit showed that the

TABLE IV
RESULTS OF RESPONSE SURFACE 2FI MODEL FOR CF

Source	Sum of squares	Degrees of freedom	Mean square	F-value	P-value	Characteristics
Model	0.06	5	0.01	77.74	< 0.0001	Significant
A-density	0.04	1	0.04	248.42	< 0.0001	
B-pressure	1.76E-004	1	1.76E-004	1.25	0.2715	
C-speed	4.64E-004	1	4.64E-004	3.30	0.0783	
D-material	0.014	1	0.014	99.96	< 0.0001	
AD	5.04E-003	1	5.04E-003	35.79	< 0.0001	
Residual	4.78E-003	34	1.41E-004			
Lack of fit	3.66E-003	24	1.53E-004	1.36	0.3150	Not significant
Pure error	1.12E-003	10	1.12E-004			
Cor total	0.06	39				

model was valid.

Index statistics, R-squared coefficient, Adj R-squared, and Pred R-squared values were 0.74, 0.68, and 0.61, respectively so the "adjusted R-squared" was close to the "predicted R-squared". The quadratic model was suggested and the model equation for CFV is presented in Eq. (9):

$$\begin{aligned} CFV = 30.20 - 36.83\times A + 21.96\times B - 15.45\times C - 2.35\times D \\ -22.17\times AB + 47.98\times A^2 - 22.62\times B^2 - 19.61\times C^2 \end{aligned} \tag{9}$$

Fig. 10 shows the interaction among the different independent variables and their corresponding effects.

As the thickness decreases due to pressure, the diameter of the yarn increases and the cross-section of the yarn becomes elliptical [27] so in all samples, the CFV increases while its slope decreases. At lower densities, there is more space to increase the diameter of the yarns. Moreover, the fewer yarn interactions (reduction of weft density) results in greater possibility of moving the fibers and yarns, so at lower densities CFV is higher as can be seen in compressibility.

At a lower speed, more compression time is applied and at constant pressure, the fabric has time to compress, which means an increase in CFV as mentioned previously in case with CF. This process is more pronounced at higher pressures and at lower densities, which is seen in Figs. 10b and 10c. Table V shows that the interaction of weft density and pressure is effective in CFV. It means that CFV in different pressures varies at each weft density.

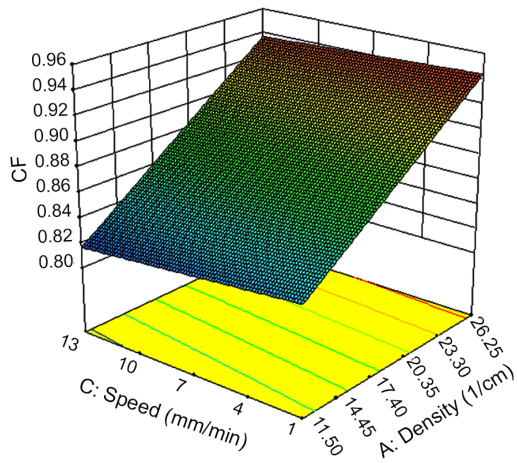

(a)

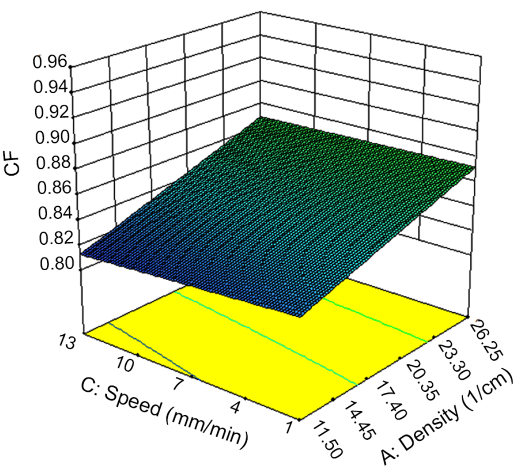

(b)

Fig. 9. Relationship between speed and weft density with CF in pressure of 364 gf/cm^2: (a) polyester fabrics and (b) viscose fabrics.

V. CONCLUSION

In this paper, the fabric compressibility, cover factor, and cover factor variation in compressed states were studied, and a suitable method for simultaneous measurement of compressibility and cover factor of fabrics was developed.

TABLE V
RESULTS OF RESPONSE SURFACE QUADRATIC MODEL FOR CFV

Source	Sum of squares	Degrees of freedom	Mean square	F-value	P-value	Characteristics
Model	62559.98	8	7820	11.24	< 0.0001	Significant
A-density	27131.11	1	27131.11	38.98	< 0.0001	
B-pressure	9646.3	1	9646.3	13.86	0.0008	
C-speed	4771.06	1	4771.06	6.85	0.0136	
D-material	220.92	1	220.92	0.32	0.5772	
AB	7866.34	1	7866.34	11.3	0.0021	
A2	12660.22	1	12660.22	18.19	0.0002	
B2	2814.34	1	2814.34	4.04	0.0531	
C2	2116.02	1	2116.02	3.04	0.0911	
Residual	21577.14	31	696.04	0.7		
Lack of fit	12866.47	21	612.69	11.24	0.7622	Not significant
Pure error	8710.67	10	871.07			
Cor total	84137.12	39				

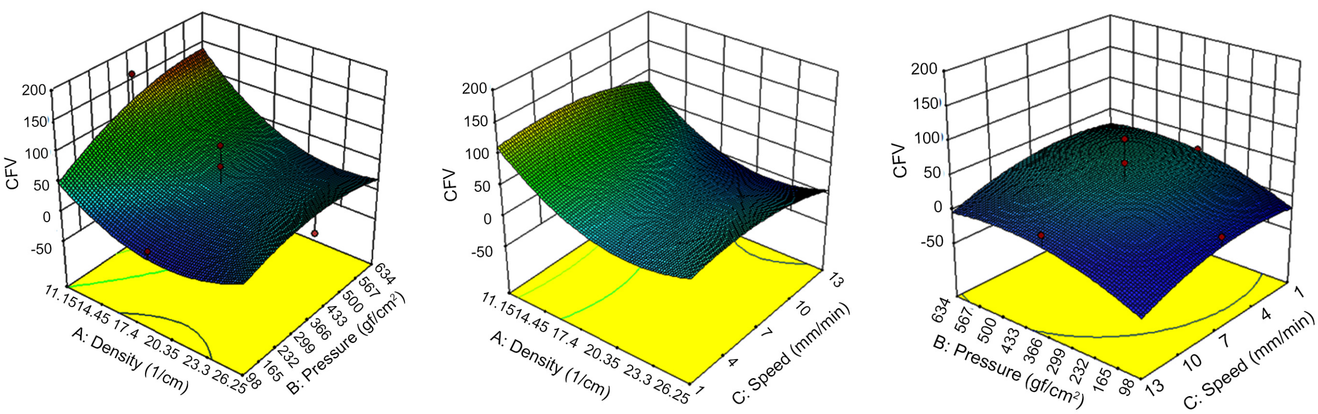

Fig. 10. (a) Relationship of pressure and density with fabric compressibility in speed of 7 mm/min, (b) relationship of speed and density with fabric compressibility in pressure of 366 gf/cm^2, and (c) relationship of speed and pressure with compressibility in density 19 (1/cm) in polyester fabrics.

The results of this research demonstrate that the behavior of fabric compressibility can be modeled through the response surface method. It was observed that by changing the weft density, the weft diameter changes more than the diameter of the warp. The weft diameter at low density is greater than the weft diameter at higher densities. The compressed fabric image was successfully processed and the cover factor was calculated with high correlation using the image processing method. With increasing pressure and decreasing density, fabric compressibility and CFV often increase. By changing weft density, compression variation range and CF are greater in polyester fabrics than in viscose fabrics. By increasing pressure, the CFV increases but the slope of the pressure-CFV curve decreases.

REFERENCES

[1] Y. Li and A.S. Wong, "Tactile Sensations", in *Association with the Textile Institut*e, Woodhead Pub, CRC, 2006.

[2] H.M. Elder, S. Fisher, K. Armstrong, and G. Hutchison, "5_fabric softness, handle, and compression", *J. Text. Inst.*, vol. 75, no. 1, pp. 37-46, 1984.

[3] J.H. Kim and S.Y. Lee, "Surface modification of PET film and fabric by oligo-chitosan treatment", *Fiber. Polym.*, vol. 15, no. 12, pp. 2489-2494, 2014.

[4] D.S. Ji and J.J. Lee, "Mechanical properties and hand evaluation of hemp woven fabrics treated with liquid ammonia", *Fiber. Polym.*, vol. 17, no. 1, pp. 143-150, 2016.

[5] J. Hu, X. Ding, and R. Wang, "Biomechanical mechanism of fabric softness discrimination", *Fiber. Polym.*, vol. 8, no. 4, pp. 372-376, 2007.

[6] J. Hu, X. Ding, R. Wang, and C. Cai, "Intrinsic differences of sensory analysis from instrumental evaluation on fabric softness by lateral compression", *Fiber. Polym.*, vol. 10, no. 3, pp. 371-378, 2009.

[7] N.S. Dhoot, L. Patil, and P. Katkar, "Effect of fabric weaves on compressional behaviour of woven fabric", *Indian J. Fibre Text. Res.*, vol. 39, no. 1, pp. 79-82, 2014.

[8] S. Uyanik and K.H. Kaynak, "Strength, fatigue and bagging properties of plated plain knitted fabrics containing different rates of elastane", *Int. J. Cloth. Sci. Technol.*, vol. 31, no. 6, 2019.

[9] S.H. Eryuruk, "The effects of elastane and finishing processes on the performance properties of denim fabrics", *Int. J. Cloth. Sci. Technol.*, vol. 31, no. 10, 2019.

[10] S. Özer, Y.E. Yüksel, and Y. Korkmaz, "Evaluation of compression-recovery and thermal characteristics of multilayer bedding textiles", *Int. J. Cloth. Sci. Technol.*, vol. 32, no. 5, 2020.

[11] A. Asayesh , M. Talaei, and M. Maroufi, "The effect of weave pattern on the thermal properties of woven fabrics", *Int. J. Cloth. Sci. Technol.*, vol. 30. no. 4, 2018.

[12] B. Behera, S. Chand, T.G. Singh, and P. Rathee "Sewability of denim", *Int. J. Cloth. Sci. Technol.*, vol. 9, no. 2, 1997.

[13] M. Akgun, B. Becerir, and H.R. Alpay, "Assessing the relationship among fabric constructional parameters, fractional reflectances and cover factors of polyester fabrics by experimental and mathematical methods", *Fiber. Polym.*, vol. 11, no. 2, pp. 291-302, 2010.

[14] A. Nazir, T. Hussain, A. Afzal, S. Faheem, and W. Ibrahim, M. Bilal "Prediction and correlation of air permeability and light transmission properties of woven cotton fabrics", *Autex Res. J.*, vol. 17, no. 1, pp. 61-66, 2017.

[15] Y. Su, R. Li, J. Yang, G. Song, and Jun Li, "Effect of compression on contact heat transfer in thermal protective clothing under different moisture contents", *Cloth. Text. Res. J.*, vol. 38, no. 1, pp. 19-31, 2020.

[16] J. Jing, "Automatic density detection of woven fabrics via wavelet transform", *J. Inform. Comput. Sci.*, vol. 11, no. 8, pp. 2559-2568, 2014.

[17] K. Yildiz, V.Y. Şenyürek, Z. Yildiz, and M.S. Özen, "A new approach to the determination of warp-weft densities in textile fabrics by using an image processing technique", *J. Eng. Fiber. Fabr.*, vol. 9, no. 1, pp. 155892501400900101, 2014.

[18] E. Shady, M. Hassan, J. Militky, and K. Qashqary, "Image processing based method evaluating fabric structure characteristics", *Fibre. Text. East. Eur.*, vol. 95, no. 6, pp. 86-90, 2012.

[19] L. Liqing, T. Jia, and X. Chen, "Automatic recognition of fabric structures based on digital image decomposition", 2008. http://nopr.niscpr.res.in/handle/123456789/2613

[20] A.I. Khuri, *Response Surface Methodology and Related Topics*, World scientific, 2006.

[21] A. Siddique, T. Hussain, W. Ibrahim, Z.A. Raza, S. Abid, and A. Nazir, "Response surface optimization in discharge printing of denim using potassium permanganate as oxidative agent", *Cloth. Text. Res. J.*, vol. 35, no. 3, pp. 204-214, 2017.

[22] M. Hadizadeh, M. Khajeh Mehrizi, and Z. Shahi, "Application of response surface methodology for modeling the color strength of natural hair colorant", *J. Text. Polym.*, vol. 7, no. 1, pp. 15-23, 2019.

[23] C.W. Choi, J.-W. Jin, H. Lee, M. Huh, and K.-W. Kang, "Optimal polymerization conditions in thermoplastic-resin transfer molding process for mechanical properties of carbon fiber-reinforced PA6 composites using the response surface method", *Fiber. Polym.*, vol. 20, no. 1, pp. 1021-1028, 2019.

[24] S. Abid, T. Hussain, A. Nazir, Z.A. Raza, A. Siddique, A. Azeem, and S. Riaz, "Simultaneous fixation of wrinkle-free finish and reactive dye on cotton using response surface methodology", *Cloth. Text. Res. J.*, vol. 36, no. 2, pp. 119-132, 2018.

[25] H. Wang, L. Xu, X. Song, and Z. Ca, "Facile preparation of acid-resistant polyester fabrics with organic/inorganic nanocomposites", *Cloth. Text. Res. J.*, vol. 35, no. 2, pp. 98-110, 2017.

[26] R.H. Yang, C.W. Kan, W.Y. Wong, and M.C. Law, "Comparative study of cellulase treatment on low stress mechanical properties of cotton denim fabric made by torque-free ring spun yarn", *Fiber. Polym.*, vol. 14, no. 4, pp. 669-675, 2013.

[27] F.T. Peirce, "5—the geometry of cloth structure", *J. Texti. Inst. Trans.*, vol. 28, no. 3, pp. T45-T96, 1937.

[28] R.N. Das, *Robust Response Surfaces, Regression, and Positive Data Analyses*, CRC Press, 2014.